

Comparative study of CO₂ Corrosion Behavior of N80, P110, X52 and 13Cr Pipe Lines in Simulated Stratum Water

Yidong Cai ^{*a}, Pengchao Guo^a, Dameng Liu^a, Shiyu Chen^b, Junlai Liu^c

^aSchool of Energy Resources, China University of Geosciences, Beijing 100083,

PR China;

^bSchool of Materials Science and Engineering, University of Science and Technology

Beijing, Beijing 100083, PR China

^cSchool of Earth Science and Resources, China University of Geosciences, Beijing

100083, PR China

Abstract: To better understand the carbon dioxide (CO₂) corrosion behavior of carbon steel and its influence on petroleum development (including drilling, production and transportation) in the Daqing Oilfield, CO₂ corrosion behaviors of N80, P110, X52 and 13Cr pipe lines in simulated solution at high temperature and high pressure condition are investigated by dynamic corrosion experiments, scanning electron microscope (SEM) and energy dispersive X-ray spectroscopy (EDX) analysis. The corrosion results reveal that the corrosion rate of all pipe lines increases quickly with the CO₂ partial pressure increasing from 0.5 MPa to 1.5 MPa, while it increases slowly with the CO₂ partial pressure increasing from 1.5 MPa to 4.5MPa, but localized corrosion is prevailing. When the experimental temperature ranges from 60 °C to 120 °C, the localized corrosion becomes very serious. The corrosion rate of all pipe lines decreased sharply for the temperature from 60 °C to

* Corresponding author. Tel.: +86-10-82320892; Fax: 86-10-82326850.
E-mail: caiyidong-2004@163.com

100 °C, it becomes stable after the temperature higher than 100 °C. As the flow rate is in the range of 0m/s-1.5m/s, the corrosion rate of sample X52 remains unchanged, while the localized corrosion gradually becomes very serious with increasing the flow rate. By analyzing the corrosion product scales of sample 13Cr, some significative phenomena were showed. When the temperature is in the range of 60 °C -100 °C, the corrosion product scales are loose and very thick, while they become very compact with increasing the temperature higher than 100 °C, localized corrosion becoming prevailing. The main components of the corrosion product scales are FeCO_3 and Cr_2O_3 .

Key words: CO_2 ; corrosion behavior; N80; P110; X52; 13Cr; Daqing Oilfield

1. Introduction

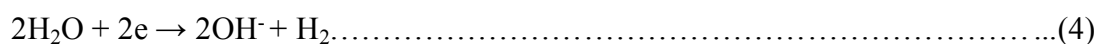
The carbon dioxide (CO_2) corrosion of steel pipe lines is very common in oil or gas fields ^[1]. As a natural phenomenon, there are many oil or gas reservoirs containing CO_2 gas in oil or gas fields, which caused many disasters and a large amount of financial loss. When the CO_2 corrosion presents, the basic feature for localized corrosion is the steel breakage, but the uniform corrosion is also normal. The corrosion rate for general corrosion is influenced by many factors (including CO_2 partial pressure, temperature, corrosion product, components of solution and steel material). But for localized corrosion, flow rate, chemical components (such as Cl^- and H_2S) and residual stress all have effect on the localized corrosion rate ^[2].

The CO_2 corrosion was studied since the 1940s in order to understand and control it ^[3]. Different types of steels have certain CO_2 corrosion features. Although low cost

carbon steels are often used as an economic material in oil production and transport

facilities, they are very susceptible to corrosion in CO₂ environments (sweet corrosion)

[4]. Several mechanisms have been proposed for interpreting the corrosion of carbon steel in CO₂-containing aqueous solution [1, 5-6], in which the main cathodic reactions can be summarized as four sub-reactions [7, 8]: H⁺ reduction as the dominant cathodic process at a lower pH value because of the high concentration of H⁺ (Eq. (1)); the direct reductions of HCO₃⁻ and H₂CO₃ become important (Eqs. (2) and (3)) when pH increases from 4 to 6; it changes to direct reduction of water (Eq. (4)) at a high over-potential.



The anodic reaction is mainly the dissolution of iron (Eq. (5)), which may be revealed through several steps as follows:



During these corrosion processes, a corrosion product (FeCO₃) would deposit on the surface of the carbon steel [9]. But, as for those carbon steels containing Cr, their product will comprise FeCO₃, Fe₃O₄ and Cr₂O₃. They have different features in

resisting further corrosion of matrix.

In this paper, based on fully considering medium parameters (including salinity, pH, Cl^- and O_2), a series of experiments considering many factors (including temperature (T), CO_2 partial pressure (P_{CO_2}), flow rate (v) and steel materials) were conducted in [Table 1](#). By analyzing and appraising each factor, their influences on CO_2 general corrosion rate and localized corrosion degree were revealed. At the same time, the different resistance of different steel material against CO_2 corrosion was discussed.

2. Experiments

2.1 Instruments and samples

The experiment instrument was developed by China University of Petroleum (CUP), which is a high temperature-high pressure dynamic corrosion autoclave (FS-III, CUP, China). The ultimate temperature and ultimate pressure of the instrument can reach at 150°C and 25 MPa, respectively.

The materials used here are commercially available N80, P110, X52 and 13Cr pipelines steel, which have different chemical composition (wt %) as shown in [Table 2](#).

These materials have different uses in oilfields. Generally, N80 steel is often used as oil tube; P110 steel used as case tube; X52 steel used as transportation pipe line of oil and gas; 13Cr steel used as well control equipment material. All of these tested samples were made with the size of 50mm (length)*10mm (width)*3mm (thickness). According to the concentration of ions in the extraction brine from simulated Daqing Oilfield conditions, Na^+ is 6095 mg/L, Ca^{2+} 24 mg/L, Cl^- 9405 mg/L, and total salinity 1.55×10^4 mg/L.

2.2 Procedures and analysis methods

All samples are polished by sandpaper, and then are cleaned by absolute alcohol. After that the samples are dried by cold dry wind, and then quickly put into the experiment instrument. Before the tests begin, the pure N₂ is poured forcedly into the solution and bubbled for 4 h, and then the pure CO₂ gas is put into autoclave. Until the pressure is up to 5 MPa, the parameters are set as follows. Temperatures ranged from 60°C to 120°C; CO₂ partial pressure from 0.5 MPa to 4.5 MPa; flow rate from 0 m/s to 1.5 m/s; the initial pH value 7.0. The test time was 24 h. In the paper, we performed these experiments following the schemes of Table 2. After the tests, take out the samples and wash them, and then clean them with absolute alcohol, dry with cold dry wind. After that, all samples are quickly weighted, so the general corrosion rate can be calculated and localized corrosion features can be analyzed as well.

Scanning electron microscopy (SEM) (Hitachi S-450, Hitachi Company of Japan) is utilized to observe the micro-morphology of the corrosion scales. Energy dispersive X-ray spectroscopy (EDX) is introduced into analyzing the elements of corrosion product scales. And then, all elements, components and structures of corrosion product scales are acquired by EDX analysis. SEM and EDX analysis are conducted at the geological lab center, China University of Geosciences in Beijing (CUGB).

3. Results and Discussions

3.1 Analysis of CO₂ corrosion under various CO₂ partial pressures (P_{CO2})

When the flow rate and temperature are set to be constant (1m/s and 120°C respectively), the influence of P_{CO2} on the general corrosion rate is discussed. Increasing

CO₂ partial pressure P_{CO2} normally induces an increase in the corrosion rate during scales-free corrosion process. After the scales formed on the steel surface, higher P_{CO2} led to an increase in CO₃²⁻ concentration and a higher supersaturation which accelerates FeCO₃ precipitation and scales growth^[10]. Generally, the corrosion rates of all three samples have a common feature with increasing P_{CO2} as shown in Fig.1. When P_{CO2} is less than 1.5 MPa, the general corrosion rate of these three samples is soaring up following the increase of P_{CO2}. N80 quickly increases from 0.03 mm/a to 2.23 mm/a, P110 from 0.03 mm/a to 1.50 mm/a, but X52 always keeps around 1.0 mm/a, which should be related with the carbon content in samples by analyzing the material. When P_{CO2} increases from 1.5 to 3 MPa, the general corrosion rate quickly decreases with increasing P_{CO2}, especially for N80, which may be related with the formation of the corrosion product scales for N80 by analyzing SEM images in Fig. 5 (a₁, 2), the corrosion product scales formed at the high temperature can resist further corrosion. When it exceeds 3 MPa, the general corrosion rate of these three samples increase with increasing P_{CO2}. The pH value will change to be small with the increase of P_{CO2}. Solution with low pH value increase corrosion with increasing the concentration of H⁺. The higher the P_{CO2} is, the lower pH value is, the quicker the depolarization is ^[11]. So, when P_{CO2} is less than 1.5 MPa, the increase of P_{CO2} will accelerate the corrosion process. The general corrosion rates slightly slows down after the P_{CO2} up to between 1.5 MPa and 3 MPa, especially for P110 and X52. At this stage, the corrosion rate indicates that the concentration of H⁺ is not the foremost factor for CO₂ corrosion process. The reason for the increase of general corrosion rates after the P_{CO2} up to 3

MPa should be the damage of corrosion product scales which controlled by stress, flow and chemical elements.

Combining SEM images with EDX analysis, the localized corrosion features, elements and scales of corrosion product can be revealed. Comparing the corrosion product scales of N80, P110, X52, we found that the scales of N80 and P110 are better than X52 under the condition of $v=1\text{m/s}$, $T=120^\circ\text{C}$ and $P_{\text{CO}_2}=1.5\text{MPa}$. Surface morphologies of CO_2 corrosion scales formed as a function of P_{CO_2} are shown. With increasing P_{CO_2} , the scales become more compact together with a reduction in the grain size of iron carbonate. At the same time, the scales thickness increases as shown in Fig. 5, Fig. 6 and Fig. 7, which can prevent the corrosion process remarkably, especially for N80 and P110. Taking N80 as an example, EDX analysis reveals that there are Fe, C, O, and Ca in the scales formed at 0.5 MPa, 1.5 MPa and 4.5 MPa. These EDX results indicate that when the P_{CO_2} is 0.5 MPa, the scales consists of CaCO_3 and FeCO_3 , while at 1.5 MPa and 4.5 MPa, the scales containing complex carbonates $(\text{Fe,Ca})\text{CO}_3$. The localized corrosion features are revealed by SEM analysis as well. 13Cr under the condition of $P_{\text{CO}_2}=0.5\text{MPa}$, 1.5MPa , temperature= 120°C , flow rate= 1m/s is investigated as shown in Fig. 4. The results show that many pittings are formed and very sharply deep in corrosion scales with increasing P_{CO_2} . The defected area of corrosion scales easily causes localized corrosion, which has been reported by Chen et al [12].

3.2 Analysis of CO_2 corrosion under various temperatures

When P_{CO_2} and flow rate are set to be constant (1.5MPa and 1m/s respectively), the

influence of the temperature on the general corrosion rate is discussed as shown in [Fig.](#)

2. The results show that the general corrosion rates of N80 and P110 have common digressive trend with increasing temperatures. Taking P110 as an example, the general corrosion rate sharply decreases from 8.99 mm/a to 2.10 mm/a with increasing the temperature from 60°C to 100°C, which may be due to the formation of thick and compact corrosion product scales with increasing the temperatures. And then, the general corrosion rate slightly increases from 2.10 mm/a to 2.14 mm/a with increasing the temperature from 100°C to 120°C, which may be caused by localized corrosion, such as pitting existed as shown in [Fig. 10](#).

The localized corrosion features, elements and scales of corrosion product are revealed by SEM images as shown in [Fig.13](#) and [Fig.14](#) and EDX analysis. The corrosion of N80 and P110 is characterized by three distinct features under various temperatures as shown in [Fig.8](#). When the temperature is lower than 60°C, FeCO_3 is the main corrosion product without adhesion; the lubricity of material surfaces is very good, which can be regard as general corrosion. When the temperature is in the range of 60°C–100°C, certain protective corrosion product scales FeCO_3 formed with increasing the temperatures and the protrusion of localized corrosion such as mesa-attack corrosion occurred as shown in [Fig. 11](#). When the temperature is higher than 100°C, the thick and compact corrosion product scales of FeCO_3 , Fe_3O_4 and little $\alpha\text{-FeOOH}$ ^[13] with strong adhesion formed. The general corrosion decreases with increasing temperatures, but the localized corrosion is very serious.

The localized corrosion for 13Cr is very serious as well. But the corrosion product

scales for 13Cr are different from that of the normal carbon steel under various temperatures as shown in Fig. 9. When the temperature is lower than 60°C, Cr^{III}-OH is the main corrosion product and is soft without strong adhesion. The lubricity of material surfaces is very good, which can be regarded as general corrosion. When the temperature ranges from 60°C to 100°C, certain protective corrosion product scales FeCO₃ and Cr^{III}-OH formed with increasing the temperature. When the temperature is higher than 100°C, the thick and compact corrosion product scales of FeCO₃, Fe₃O₄ and Cr^{III}-OH with strong adhesion formed.

3.3 Analysis of CO₂ corrosion under various flow rates

When the temperature and P_{CO2} were set to be constant (120°C and 1.5MPa respectively), the influence of the flow rate on the general corrosion rate for X52 was discussed as shown in Fig. 3. Increasing flow rate will result in the increase of pervasion speed of HCO₃⁻ and H⁺, which caused the velocity of corrosion medium to speed up to get to the surface of material more easily and strengthened the depolarization of cathodes. At the same time, the Fe²⁺ will be taken away by flow fluid, which resulted in the increase of corrosion rate. And high flow rate would restrain the formation of corrosion product scales effectively, which will turn to be very complex as shown in Fig.3. Overall, the general corrosion rate kept around 1.0mm/a.

Some interesting phenomena of localized corrosion features, elements and scales of corrosion product were revealed by SEM images and EDX analysis. Taking X52 as an example, when the flow rate is less than 1.0m/s, FeCO₃, Fe₂O₃, MoO₃ and MoC are the main product scales, which are revealed by EDX analysis. When the flow rate is larger

than 1.0m/s, FeCO_3 is the main corrosion product scales and is little as shown in [Fig.12](#).

Eroded channels are very normal, which performs as a type of localized corrosion. The long and deep eroded channels exist in materials surface. These entire situations always happened along the defected district of carbon steel material. The localized corrosion for X52 is very serious because of the material components as shown in [Table 2](#). There is no Cr existed in X52 carbon steel material, which resulting in the most serious localized corrosion.

3.4 Analysis of CO_2 corrosion under various corrosion product scales

When flow rate, temperature and P_{CO_2} were all set to be constant (1m/s, 120°C and 1.5MPa respectively), the influence of corrosion product scales for different steel materials (including N80, P110, X52, 13Cr) on general corrosion rate was discussed. In CO_2 -containing environment, the components, structures, morphology and features of corrosion product scales were mainly influenced by medium, P_{CO_2} , temperatures and materials. In our research, the components of the main corrosion product scales are $(\text{Ca,Fe})\text{CO}_3$, Fe_2O_3 , Cr_2O_3 and other alloy with oxide. In some special material, some particular elements such as Cr, Mo existed in 13Cr, which resulting in the formation of special corrosion product scales MoO_3 and MoC approved by EDX analysis. By investigating SEM images and EDX, the localized corrosion features, elements and scales of corrosion product were revealed vividly.

3.4.1 Corrosion product scales under various temperatures

Based on the research, the corrosion product scales of normal carbon steels were seriously affected under various temperatures. The [Fig.16](#) revealed the changed

thickness and compaction of corrosion product scales with increasing temperatures. At the same time, some elements in scales also changed with the temperatures, such as Ca in corrosion scales of P110 as shown in Fig.17. The thickness of corrosion product scales increased with increasing temperatures as shown in Fig 17. In high temperature, FeCO_3 and Fe_3O_4 easily formed in N80 and P110 because of the function of H^+ and Fe^{2+} , which caused thick and compact corrosion scales formed. The corrosion scales that are integrated and compacted with strong adhesion can effectively slow down the general corrosion, but the corrosion scales with defects can induce the serious localized corrosion.

3.4.2 Corrosion product scales under various flow rates

At the present flow rate ranging from 0 to 1.5 m/s, at initial corrosion stage there was no scales formed on the steel, the flow enhanced the general corrosion rather than localized corrosion because of the facilitated mass transfer process [14] with fewer corrosion reactions accumulating on the steel surface.

Fig. 18(a₁) indicates that the scales thickness increased with increasing flow rate. At the same time, the scales became denser, as shown in Fig. 12, especially in the area near the interface between the scales and steel. However, the corrosion rate at high flow rates was greater than that in the static state, which implied that the thicker and denser scales did not protect the steel effectively. Crolet [15] pointed out that the protective ability of corrosion scales depended on the structure and morphology of the scales instead of its thickness. With regards to the ion permeation mechanism, a thicker and denser scale is beneficial to restrain the CO_2 corrosion process, but is not the

controlling factor ^[16]. At the initial corrosion stage only when corrosion scales formed very densely with good mechanical properties as well as resistance to anions permeation does it protect the steel effectively.

EDX analysis confirmed the presence of Fe, C, O and Ca under static condition. Ca was found in all scales, and the variation of the amount of Ca with respect to flow rate was shown in Fig. 18(a₂). This phenomenon should be attributed to complex carbonates (Fe,Ca)CO₃ formed in the scales under dynamic and static conditions, respectively ^[17].

3.4.3 Corrosion product scales under various materials

In this paper, we mainly discuss the influence of Cr content on the corrosion scales. The Cr content in N80 and P110 is low, while it's high in 13Cr and no in X52 as shown in Table 2. Based on the experiments, the relationship between Cr and general corrosion rate is revealed. As shown in Fig.15, the general corrosion increases with the Cr content increasing. That may be different from our general thinking which considers high content of Cr can form thick and compact scales, but actually, high Cr-contained scales are easily destroyed as well. So, it cannot well prevent the corrosion with the Cr content lower than 13%. But compared with common carbon steel, steel with Cr element is still better than others in resisting corrosion.

4. Conclusions

Under different conditions, corrosion features are different. From the point of view of materials, the general corrosion rate is P110>N80>X52, the degree of localized corrosion is X52>P110>N80, the advantage of corrosion product scales is

13Cr>N80>P110>X52. From the point of P_{CO_2} , the general corrosion rate is variable under different conditions, which basically increases first and then goes down. Localized corrosion is pervasive and very serious at high CO_2 partial pressure. Overall, higher the P_{CO_2} is, more serious the localized corrosion is. The formation of the best corrosion product scales varies with different materials. Judging from the temperature, the general corrosion rate decreases with increasing the temperatures. The localized corrosion at low temperatures is more serious than that at high temperatures because of corrosion scales. From the point of view of flow rate, the general corrosion rates are variable under different flow rates, basically like wave style. There are no special features existing. The localized corrosion turns to be very serious with increasing the flow rate.

Based on this research, the carbon steel with Cr should be used and the CO_2 partial pressure minimized during the oil or gas production for reducing the corrosion in the oilfield. For considering the corrosion product scales, the flow rate in transportation should be lower than 1.5 m/s.

Acknowledgements

This study was financially supported by the Daqing Oilfield Limited Company of PetroChina (DQYT-0404003-2008-JS-963).

References

- [1] M.B. Kermani and A. Morsed, Corrosion/59, (2003): 659.
- [2] Y.D. Cai, L. Zhou, J.X. Li, D.M. Liu, Corrosion and Protection/29, (2008): 526-529.
- [3] A. Ikeda, M. Ueda, and S. Mukai, Corrosion/83, (1983): 45.

- [4] J.L. Crolet, Predicting CO₂ corrosion in oil and gas industry, Proceedings from 10th European Corrosion, Progress in the Understanding and Prevention of Corrosion/1, Paper No.1, Institute of Materials, London, 1994.
- [5] K. Videm, J. Kvarekval, Corrosion/51, (1995): 260.
- [6] T. Hong, Y.H. Sun, W.P. Jepson, Corrosion Sciences/44, (2002):101.
- [7] G.I. Ogundele, W.E. White, Corrosion/42, (1986): 71.
- [8] S. Nesic, J. Postlethwaite, S. Olsen, Corrosion/52, (1996): 280.
- [9] D.A. Lopez, W.H. Schreiner, S.R. de Sanchez, S.N. Simison, Applied Surface Sciences/207, (2003): 69.
- [10] S. Nesic, K.-L.J. Lee, Corrosion/59, (2003): 616-628.
- [11] A.K. Dunlop, NACE Corrosion/83, (1983): 46.
- [12] C.F. Chen, M.X. Lu, G. X. Zhao, Z.Q. Bai, M.L. Yan, Y.Q. Yang, Acta Metallurgica Sinica/38, (2002): 411-416.
- [13] D.G. Li, Y.R. Feng, Z.Q. Bai, M.S. Zheng, Applied Surface Science/253, (2007): 8371-8376.
- [14] E. Dayalan, F.D. de Moraes, J.R. Shadley, S.A. Shirazi, E.F. Rybicki, NACE Corrosion/98, (1998): 51.
- [15] J.L. Crolet, M.R. Bonis, Corrosion/39, (1983): 39-46.
- [16] K.W. Gao, F. Yu, X.L. Pang, G.A. Zhang, L.J. Qiao, W.Y. Chu, M.X. Lu, Corrosion Sciences/50, (2008): 2796-2803.
- [17] S. Wu, Z. Cui, F. He, Z. Bai, S. Zhu, X. Yang, Mater. Lett. /58, (2004): 1076-1081.